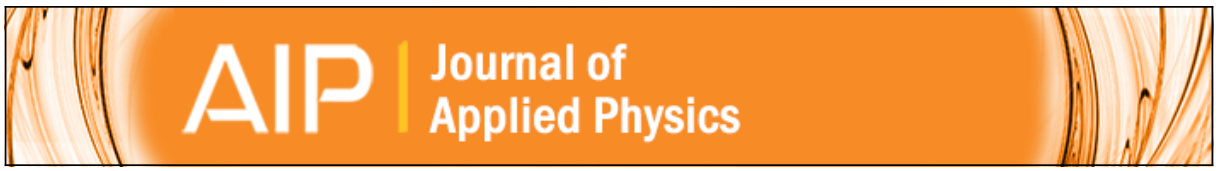


# Influence of electric fields on the depolarization temperature of Mn-doped (1-x)Bi1/2Na1/2TiO3-xBaTiO3

Eva Sapper, Silke Schaab, Wook Jo, Torsten Granzow, and Jürgen Rödel

Citation: Journal of Applied Physics **111**, 014105 (2012); doi: 10.1063/1.3674275
View online: http://dx.doi.org/10.1063/1.3674275
View Table of Contents: http://scitation.aip.org/content/aip/journal/jap/111/1?ver=pdfcov
Published by the AIP Publishing



# Influence of electric fields on the depolarization temperature of Mn-doped (1-x)$Bi_{1/2}Na_{1/2}TiO_3$-x$BaTiO_3$

Eva Sapper,[a] Silke Schaab, Wook Jo, Torsten Granzow, and Jürgen Rödel
*Institute of Materials Science, Technische Universität Darmstadt, Darmstadt 64287, Germany*

(Received 15 June 2011; accepted 6 December 2011; published online 6 January 2012)

The transition between induced long-range order and relaxor-like behavior upon heating is investigated in lead-free (1-x)$Bi_{1/2}Na_{1/2}(Ti_{0.995}Mn_{0.005})O_3$-x$Ba(Ti_{0.995}Mn_{0.005})O_3$ piezoceramics with $x = 0.03$, 0.06, and 0.09 (BNT-100xBT:Mn). Temperature-dependent permittivity $\varepsilon'(T)$ and thermally stimulated depolarization currents (TSDC) of poled samples were measured under identical heating conditions to clarify the depolarization mechanism. In both methods, the influence of electric bias fields on the transition temperature was investigated. Fields applied in the poling direction shift the transition to higher temperatures, with corresponding results in $\varepsilon'(T)$ and TSDC measurements. While the response of transition temperature to external fields displays a similar trend in all investigated compositions, the shape of TSDC is clearly connected with the composition and, hence, the crystal symmetry of the sample. Furthermore, the comparison of $\varepsilon'(T)$ and TSDC data reveals a systematic shift between transition temperatures obtained with the two different methods. © *2012 American Institute of Physics*. [doi:10.1063/1.3674275]

## INTRODUCTION

The market for piezoelectric sensor and actuator applications is currently still dominated by lead-containing materials, such as lead zirconate titanate (PZT).[1,2] The need to replace lead has raised interest in the lead-free piezoceramic (1-x)$Bi_{1/2}Na_{1/2}TiO_3$-x$BaTiO_3$ (BNT-100xBT), whose promising piezoelectric behavior is attributed to the existence of a morphotropic phase boundary (MPB) similar to that of PZT.[3,4] Manganese doping further improves the material properties by reducing conductivity and enhancing the piezoelectric coefficient, which increases the potential for actuator applications.[5]

The discovery of an MPB[3] in BNT-100xBT for $x = 0.06 \sim 0.07$ resulted in a lot of research on phase stability regions and related electrical properties of the material with compositions in the vicinity of the boundary.[6,7] A recent study by Jo *et al*. points toward the existence of R3m symmetry in the unpoled material, which is transformed to a mixture between R3c and P4m(b)m on poling.[7] Neutron diffraction investigations by Simons *et al*.[8] indicate that both R3c and P4bm symmetries exist, even at the unpoled state, with a very slight lattice distortion. Poling induces predominantly rhombohedral distortion with a pronounced preferred orientation along the field direction.[8] The doping of BNT-6BT with manganese up to 0.45 wt. % decreases the lattice constant without changing the overall crystal structure.[9]

A field-induced structural change is reflected in the dielectric properties of BNT-100xBT as well. The dielectric permittivity $\varepsilon'(T)$ of unpoled samples is characterized by a broad permittivity maximum and a strong frequency dispersion in the low-temperature regime.[10] These properties indicate relaxor behavior[11–14] rather than the initially proposed ferroelectric-antiferroelectric transition.[3] In poled BNT-100xBT samples, the frequency dispersion as well as the absolute value of the permittivity in the low-temperature regime is clearly reduced, indicating a field-induced long-range order.[15] Again, this is similar to the findings in the conventional relaxors $Pb_{0.92}La_{0.08}(Zr_{0.65}Ti_{0.35})_{0.23}O_3$ (PLZT 8/65/35) and $Pb(Mg_{1/3}Nb_{2/3})O_3$ (PMN).[14,16] In these well-described relaxor materials, the frequency dependence of $\varepsilon'(T)$ is attributed to the existence of polar nanoregions (PNRs) within a nonpolar matrix. The assumption of a relaxor mechanism in BNT-100xBT is supported by the discovery of nanometer-size polar regions in diffuse scattering[17] and TEM analysis.[18] Furthermore, the existence of PNRs with a maze-like domain pattern has been observed by piezoresponse force microscopy[19] in BNT-5.5BT and by TEM[19] in Mn-doped BNT-5.5BT. Relaxor properties of permittivity[20,21] and the existence of a microdomain configuration[22] have been reported for other BNT-based solid solutions as well.

The correlated relaxation of the PNRs in an external AC-field gives rise to the observed dielectric dispersion.[23] While normal ferroelectrics undergo a spontaneous phase transition from a paraelectric state to a ferroelectric order upon cooling, PNRs in many relaxors do not percolate throughout the whole sample upon cooling. In contrast, they freeze from a high temperature ergodic relaxor state to a low-temperature nonergodic state[24] without macroscopically discernable symmetry change.[12] In the nonergodic state, a ferroelectric long range order can often be induced by a sufficiently large electric field. Upon heating, the induced long range order decays at the ferroelectric-to-relaxor transition temperature $T_{F\text{-}R}$[25] and the frequency dispersion is recovered. In the real and imaginary part of the temperature-dependent permittivity $\varepsilon'(T)$ and $\varepsilon''(T)$, respectively, this temperature is marked by a frequency invariant anomaly. With respect to the application of BNT-100xBT as a piezoelectric actuator material, detailed

[a]Author to whom correspondence should be addressed. Electronic mail: sapper@ceramics.tu-darmstadt.de.

 

information on the temperature of depolarization $T_d$ and the underlying mechanism of the transition are necessary for the application and further improvement of BNT-100xBT:Mn piezoceramics. A high $T_d$ is desirable to extend the possible range of application temperatures. For the "classic" relaxor materials, PLZT 9/65/35 (Ref. 26) and PMN,[27] it has been shown that an electric field in the poling direction can delay the depolarization during heating.

Commonly, $T_{F\text{-}R}$ obtained from $\varepsilon'(T)$ measurements is assumed to be identical to the depolarization temperature $T_d$,[28,29] as thermally stimulated depolarization currents (TSDC) and data on the temperature dependence of the piezoelectric coefficient $d_{33}(T)$ have been found to correspond well with permittivity data for PLZT[30,31] and $BaTiO_3$.[32] However, the physical correlation between increasing permittivity and the actual depolarization of relaxor materials is still not clarified, and a comparison of different methods by Anton *et al.* indicates a systematical shift between $T_{F\text{-}R}$ determined from $\varepsilon'(T)$ and $T_d$ determined from TSDC or $d_{33}(T)$ measurements.[33] In contrast to permittivity measurements, the TSDC method[31,32,34–36] is able to detect depolarization directly by measuring resulting currents.

In this study, the common $\varepsilon'(T)$ measurement is correlated with TSDC data in BNT-100xBT:Mn samples with different phase content to gain further insight into the mechanisms of depolarization. The focus lies on the possibility to shift the depolarization to higher temperatures to extend the temperature range of application.

## EXPERIMENTAL SETUP

BNT-100xBT:Mn ceramics with $x = 0.03$, 0.06, and 0.09 and 0.5 mol. % $MnO_2$ content were prepared by a conventional mixed oxide method using $Bi_2O_3$ (99.975% purity), $Na_2CO_3$ (99.5%), $BaCO_3$ (99.8%), $TiO_2$ (99.9%), and $MnO_2$ (99.9%, all powders by Alfa Aesar, Karlsruhe, Germany) as raw materials. The starting materials were weighed according to the stoichiometric formula and ball-milled for 24 h in ethanol. The dried slurries were calcined at 900 °C for 3 h and then ball milled again for 24 h. The powders were subsequently pressed into green disks with a diameter of 10 mm. Sintering was carried out at 1150 °C for 3 h in covered alumina crucibles. To prevent evaporation of volatile elements during sintering, the samples were embedded in atmospheric powder of the same composition. The purity and formation of the desired single perovskite phase in the calcined powders and sintered products was confirmed by x-ray diffraction.

The samples were ground to approximately 300 $\mu$m, polished, and electroded with sputtered silver. An additional electrode layer of silver paste (Gwent Electronic Materials, Pontypool, UK) was fired on to assure mechanical and thermal stability. Prior to every measurement the samples were annealed for two hours at 450 °C to rule out aging effects.

Samples were poled for 5 min under a DC field of 6 kV/mm at room temperature directly before the measurements. The comparison with the remanent polarization $P_r$ obtained from polarization hysteresis measurements confirmed that this field was sufficient to pole the samples. If a DC field was applied during the measurement, its direction was always parallel to that of the field used for poling.

Dielectric measurements were carried out with a HP4284A impedance analyzer using a Nabertherm furnace at a constant heating rate of 2 K/min and frequencies from $10^2$ Hz to $10^5$ Hz. Real part $\varepsilon'$ and imaginary part $\varepsilon''$ of the temperature-dependent dielectric permittivity were calculated from the measured capacitance using the known sample thickness $h$ and surface area $A$.

Dielectric measurements under DC field were carried out at 1 kHz with a small signal measurement setup. Upon heating, a constant DC field was applied using a FuG 2000 V high voltage source (Rosenheim, Germany). In addition, a small signal AC field with an amplitude of 15 V/mm was applied. The incremental polarization change was detected using a Stanford Research Systems SR 830 Lock-In amplifier (Sunnyvale, CA) combined with a conventional Sawyer-Tower setup.

Thermally stimulated depolarization currents $I(T)$ were detected with a Keithley 6517B ampere meter. Poled samples were heated at a rate of 2 K/min. For measurements with offset fields, a high voltage source was connected in series with the sample, and different DC bias fields between 200 V/mm and 600 V/mm were applied during heating.

The temperature-dependent polarization $P(T)$ was calculated from the depolarization current according to Eq. (1),

$$P = \int j(T)dT = \int \frac{I(T)}{A} dT. \tag{1}$$

Additionally, $T_d$ was determined from the maximum in $j(T)$, i.e., $T_d$ is the inflection point of $P(T)$ according to Eq. (1).[33]

## RESULTS

Figure 1 provides the temperature-dependent permittivity $\varepsilon'(T)$ and loss factor $\varepsilon''(T)$ of poled BNT-3BT:Mn, BNT-6BT:Mn, and BNT-9BT:Mn measured upon heating. In all compositions, the $\varepsilon'(T)$ curves display a broad maximum at high temperatures over a wide temperature range. The temperature of the absolute maximum of $\varepsilon'(T)$ is around 300 °C for all three compositions. In the same region, one can observe a maximum of the loss factor $\varepsilon''(T)$, with a very pronounced frequency dispersion. This maximum gets more pronounced with increasing $BaTiO_3$ content and was recently attributed to a second relaxor contribution.[25] There is a further, frequency independent, anomaly of the permittivity at lower temperatures that marks the transition from the ferroelectric to the relaxor state, but unlike normal ferroelectrics or even most relaxors, it does not present a clear maximum. To obtain an unambiguous criterion for the quantitative determination of $T_{F\text{-}R}$, the maximum of the first derivative of the permittivity is chosen as the transition point.[33] Around $T_{F\text{-}R}$, $\varepsilon''(T)$ has a maximum. The order of the maxima at different frequencies is inversed compared to the maxima near $T_m$: high measurement frequencies result in lower values of $\varepsilon''$. In contrast to $T_m$, $T_{F\text{-}R}$ varies strongly with composition. The effect of the transition is most pronounced for BNT-6BT:Mn. Of the three samples, it has the lowest

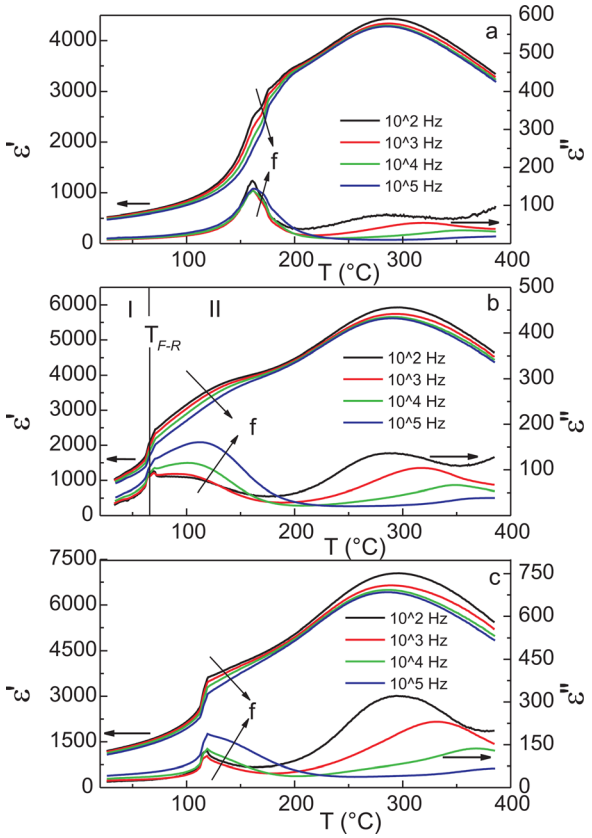


FIG. 1. (Color online) Temperature-dependent permittivity of poled samples upon heating with 2 K/min. (a) BNT-3BT:Mn, (b) BNT-6BT:Mn, (c) BNT-9BT:Mn. Arrows indicate increasing measurement frequency from $10^2$ Hz to $10^5$ Hz.

transition temperature of $T_{F\text{-}R} = 65\,^{\circ}\text{C}$. In this sample, the transition divides the $\varepsilon'(T)$ and $\varepsilon''(T)$ curves into two parts. In region I, below $T_{\text{F-R}}$, $\varepsilon'(T)$ and $\varepsilon''(T)$ depend only weakly on the measuring frequency. In region II, above $T_{\text{F-R}}$, the permittivity and the dissipation factor vary with changing measurement frequency. While $\varepsilon'(T)$ in region II decreases with increasing frequency $f$, $\varepsilon''(T)$ increases with $f$ in this temperature region. For the two other samples, the effect is less pronounced; still, $T_{\text{F-R}}$ in each material is independent of the measurement frequency.

A closer look at the vicinity of the transition at $T_{\text{F-R}}$ reveals that the increase of permittivity upon heating does not take place abruptly, but is spread out over a region of approximately 8 °C in BNT-6BT:Mn. This is clearly visible in Fig. 2(a), which shows $\varepsilon'(T)$ recorded at 1 kHz for BNT-6BT:Mn under zero bias field. The transition region is marked by dashed vertical lines. The TSDC density $j(T)$ under zero bias is shown in Fig. 2(b), along with the polarization calculated according to Eq. (1). The depolarization current displays a broad, diffuse peak structure with two maxima. It is noted that the width of this peak is identical with that of the transition region in $\varepsilon'(T)$, but $T_{\text{d}}$, determined from the first maximum of the current, is about 8 °C lower than $T_{\text{F-R}}$. The maximum polarization in the field-induced low temperature phase calculated by integrating the current is 38 $\mu$C/cm$^2$ (Fig. 2(b)). This is consistent with a remanent polarization of 40 $\mu$C/cm$^2$ obtained from $P(E)$ hysteresis measurements.

The influence of external bias fields in the poling direction is displayed in Figs. 2(c)-2(h) for BNT-6BT:Mn. The application of external fields during heating clearly shifts the transition region to higher temperatures. This shift was detected both in $\varepsilon'(T)$ and $j(T)$, and the degree of the shift was the same in both types of measurement. The width of the transition region does not change with increasing field.

Figure 3 shows the comparison of $\varepsilon'(T)$ and the depolarization current density $j(T)$ at different bias fields for all three levels of BT-doping. The field-induced shift already described for BTN-6BT:Mn occurs in BNT-3BT:Mn and BTN-9BT:Mn as well, although the degree of shift depends on the composition. Interestingly, the character of the TSDC maximum also changes with composition. For rhombohedral phase BNT-3BT:Mn, the TSDC peak consists only of a single maximum. BNT-6BT:Mn exhibits two maxima and, in BNT-9BT:Mn, the depolarization current has a rather diffuse structure with multiple maxima. In any case, $T_{\text{d}}$ was determined from the first maximum of $j(T)$. In all investigated compositions, $T_{\text{d}}$ is lower than $T_{\text{F-R}}$. To rule out artifacts from temperature gradients within the different furnaces, measurements with external thermo-couples and different heating rates were carried out. No divergence explaining the observed temperature deviation was found.

## DISCUSSION

The wide permittivity maximum and frequency dispersion above $T_{\text{F-R}}$, which appear in all investigated compositions of BNT-100xBT:Mn (Fig. 1), indicate relaxor behavior. The reduced dispersion below $T_{\text{F-R}}$ points toward a field-induced long range order, which decays upon heating. This correlates well with the occurrence of ferroelectric $P(E)$ hystereses below $T_{\text{F-R}}$, which become more and more constricted with heating above $T_{\text{F-R}}$.[37] We assume that the induced ferroelectric state is stable upon heating until $T_{\text{F-R}}$ is reached, where the long range order breaks up and the material converts to its original short-range ordered state. The recovery of PNRs gives rise to the frequency dispersion above $T_{\text{F-R}}$.

Figure 2 shows that the ferroelectric to relaxor transition in BNT-100xBT:Mn can be modulated by external fields well below the coercive field. Both $T_{\text{F-R}}$ and $T_{\text{d}}$ are clearly affected by the external bias. Obviously, the temperature range of ferroelectric behavior can be extended by external bias fields. This is in agreement with acoustic emission data obtained from undoped BNT-6BT, which shows that a field of 850 V/mm can induce long-range order and remanent polarization, respectively, at 140 °C.[38]

The diffuse maxima observed in the TSDC of BNT-6BT:Mn and BNT-9BT:Mn in contrast to BNT-3BT:Mn (Fig. 3) indicate that the stepwise depolarization is a result of the mixed phase structure. Colla and Weissmann reported a similar feature for the temperature-induced depolarization of the relaxor material $(PbMg_{1/3}Nb_{2/3}O_3)_{0.94}(PbTiO_3)_{0.06}$ (PMN-0.06PT)[39] and related it to the existence of different types of PNRs. Assuming that BNT-100xBT:Mn is a relaxor, the coexistence of tetragonal and rhombohedral PNRs with different transition temperatures might be suggested for

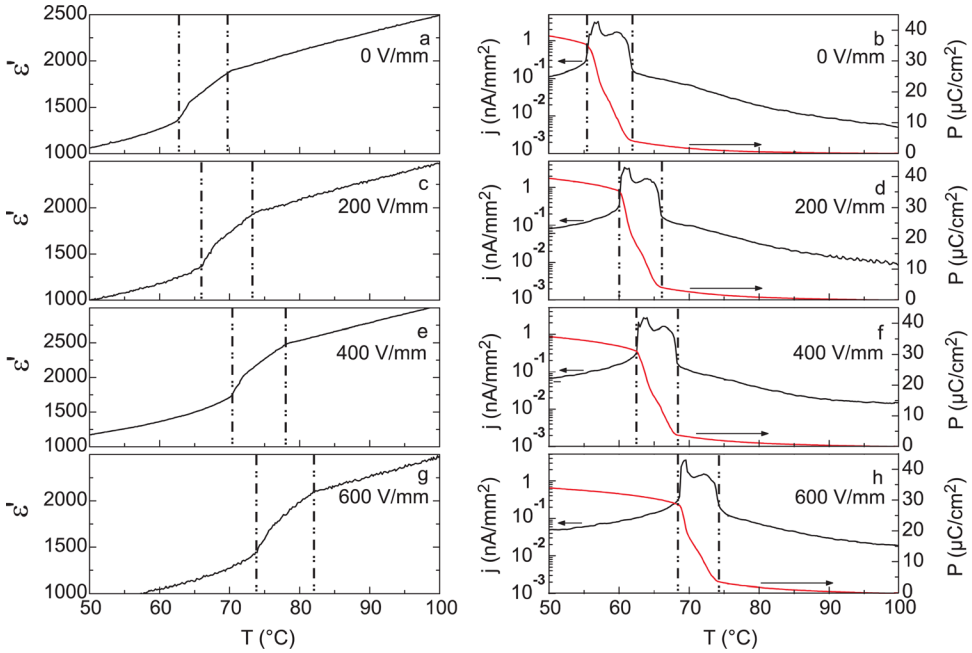


FIG. 2. (Color online) BNT-6BT:Mn, permittivity in the transition region measured at 1 kHz with different bias fields (a, c, e, g) and thermally stimulated depolarization current and polarization loss with different bias fields (b, d, f, h). Vertical lines indicate the width of the transition region.

BNT-6BT:Mn. This picture is in agreement with neutron diffuse scattering investigations on $(PbZn_{1/3}Nb_{2/3}O_3)_{0.92}(PbTiO_3)_{0.08}$ single crystals by Gehring *et al.*[40] They have shown the existence of tetragonal and orthorhombic PNRs, which align differently in external fields and, therefore, can be assumed to be the origin of different transition temperatures.

Nevertheless, the origin of the diffuse peak shape in BNT-9BT:Mn remains unclear. Studies on the lead-containing relaxor $(PbMg_{1/3}Nb_{2/3}O_3)_{0.88}(PbTiO_3)_{0.12}$ report an increasing diffuseness of the TSDC peak, with aging time[41] similar to that in BNT-9BT:Mn. Even though all samples were annealed before the measurements, aging during cooling and the measurement itself cannot be completely excluded. Comparisons of aging behavior in different compositions are needed to elucidate the influence of aging on depolarization.

In Fig. 4, the influence of external fields on $T_{F\text{-}R}$ and $T_d$ is compared for all investigated compositions. For BNT-6BT:Mn and BNT-9BT:Mn, an overall linear influence of the external field on the transition temperature is observed, with the effect being larger in BNT-9BT:Mn. In BNT-3BT:Mn, $T_{F\text{-}R}$ does not exhibit a notable dependence on the external field, but $T_d$ again increases nearly linearly. Like the shape of the TSDC peaks, this finding can be attributed to the crystal structure if there are two different types of PNRs which differ in their reaction to the applied field. The shift of $T_d$ is due to the stabilization of macroscopic polarization by the external field in the poling direction. This occurs in all three compositions examined and, in fact, in all ferroelectrics. $T_{F\text{-}R}$ does not depend on the macroscopic polarization, but the long-range interaction between the local dipoles. In BNT-3BT:Mn, the structure is predominantly rhombohedral; the fraction of tetragonal phase increases with increasing BT content. The results indicate that the external field stabilizes the long-range interaction between the dipoles in domains in the tetragonal phase, but not the rhombohedral phase. However, this picture remains hypothetical, and further investigations on the structure of PNRs are needed.

In addition, the fact that $T_d$ is lower than $T_{F\text{-}R}$ in all compositions is displayed clearly in Fig. 4. In literature, a similar trend is found by comparing data obtained from temperature-dependent permittivity and temperature-dependent $d_{33}$. The depolarization temperatures from $d_{33}(T)$ are always lower than transition temperatures determined from permittivity

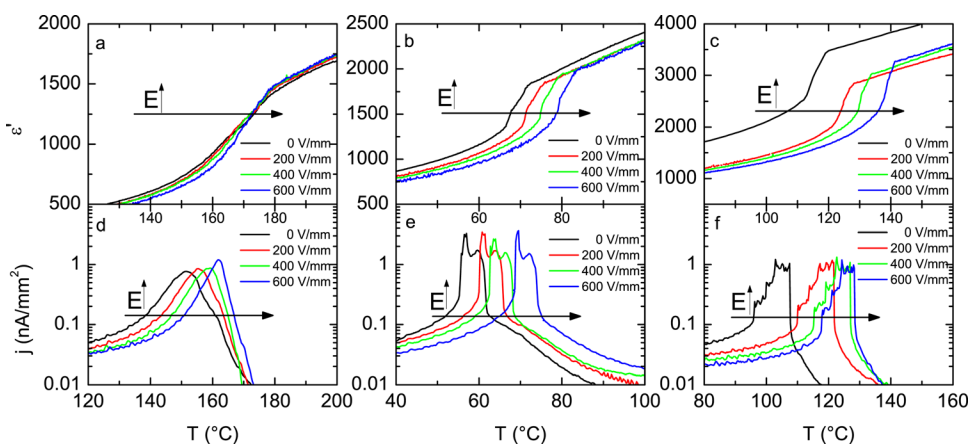


FIG. 3. (Color online) Influence of bias field on permittivity (at 1 kHz) and TSDC of poled samples: (a) BNT-3BT:Mn, (b) BNT-6BT:Mn, (c) BNT-9BT:Mn.

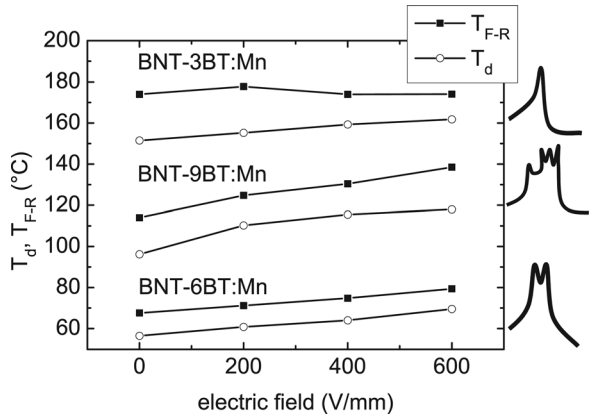


FIG. 4. Influence of bias field on depolarization temperature $T_d$ from TSDC (open symbols) and transition temperature $T_{F\text{-}R}$ from permittivity (closed symbols).

data.[33] Therefore, we suggest that loss of polarization and increase of permittivity in BNT-100xBT:Mn are due to discrete origins. Heating above $T_d$ destroys the macroscopic polarization. The orientation of the domains starts to fluctuate due to thermal activation, but the coherence of the local dipoles within the domains is not lost. The domains break up into PNRs only when the material is heated to $T_{F\text{-}R}$ and above. The resulting increase in domain wall density causes the observed maximum in the permittivity.[42] In other words, even though the macroscopic domain structure decays at $T_d$, the coherence of the dipoles within the domains does not. Instead, it extends slightly into the region of the unpoled sample. A similar effect has been found in the classical ferroelectric PZT. In soft PZT, a long-range order can be identified with x-ray diffraction, even at temperatures where the remanent polarization is negligible. The fact that the polarization loss occurs at lower temperatures than the decay of the long-range order was explained by the existence of depolarizing fields and stresses due to mismatch between grains.[43]

With respect to most applications, the depolarization temperature $T_d$ is the relevant parameter, since the piezo- and pyroelectric effect depends less on long-range order between local dipoles and more on the possibility to retain a macroscopic remanent polarization. This temperature can be enhanced in all compositions investigated by applying an external field; in this way, it is therefore possible to extend the temperature range where the material can be used in applications. When determining the depolarization temperature from any other method, it is important to keep in mind that different methods probe for different physical phenomena. One has to make sure that the specific method chosen is really sensitive to the loss of macroscopic polarization indicated by $T_d$ and not, e.g., the loss of long-range order between dipoles indicated by $T_{F\text{-}R}$.

## CONCLUSIONS

In BNT-100xBT:Mn around the MPB, depolarization during heating ($T_d$) occurs before ferroelectric order breaks down ($T_{F\text{-}R}$). Mn-doping decreases $T_{F\text{-}R}$ by about 20 °C compared to undoped samples.[25] Electric bias fields in the poling direction are able to shift the depolarization of all investigated materials to higher temperatures. The depolarization current depends strongly on phase composition and points to the existence of both rhombohedral and tetragonal nanopolar regions. These results give further insight into the possibility of driving actuators above $T_d$. Furthermore, they indicate the feasibility of extending the working temperature range of lead-free BNT-100xBT:Mn by applying comparably low bias fields.

## ACKNOWLEDGMENTS

This work was financially supported by the Deutsche Forschungsgemeinschaft DFG under SFB 595.

[1]P. K. Panda, J. Mater. Sci. **44**, 5049 (2009).
[2]J. Rödel, W. Jo, K. T. P. Seifert, E. M. Anton, T. Granzow, and D. Damjanovic, J. Am. Ceram. Soc. **92**, 1153 (2009).
[3]T. Takenaka, K. Maruyama, and K. Sakata, Jpn. J. Appl. Phys. **30**, 2236 (1991).
[4]Y. Hiruma, H. Nagata, and T. Takenaka, J. Appl. Phys. **104**, 124106 (2008).
[5]E. Aksel, P. Jakes, E. Erdem, D. M. Smyth, A. Ozarowski, J. van Tol, J. L. Jones, and R. D.-A. Eichel, J. Am. Ceram. Soc. **94**, 1363 (2011).
[6]Y. Hiruma, Y. Watanabe, H. Nagata, and T. Takenaka, Key Eng. Mater. **350**, 93 (2007).
[7]W. Jo, J. E. Daniels, J. L. Jones, X. Tan, P. A. Thomas, D. Damjanovic, and J. Rödel, J. Appl. Phys. **109**, 014110 (2011).
[8]H. Simons, J. Daniels, W. Jo, R. Dittmer, A. Studer, M. Avdeev, J. Rödel, and M. Hoffman, Appl. Phys. Lett. **98**, 082901 (2011).
[9]X.-J. Li, Q. Wang, and L. Quan-Lu, J. Electroceram. **20** (2008).
[10]B. Wylie-van Eerd, D. Damjanovic, N. Klein, N. Setter, and J. Trodahl, Phys. Rev. B **82**, 104112 (2010).
[11]G. A. Samara, J. Phys.: Condens. Matter **15**, R367 (2003).
[12]L. E. Cross, Ferroelectrics **76**, 241 (1987).
[13]Z. G. Ye, Key Eng. Mater. **155-156**, 81 (1998).
[14]A. Bokov and Z. G. Ye, J. Mater. Sci. **41**, 31 (2006).
[15]Y. Hiruma, K. Yoshii, H. Nagata, and T. Takenaka, Ferroelectrics **346**, 114 (2007).
[16]O. Bidault, M. Licheron, E. Husson, and A. Morell, J. Phys.: Condens. Matter **8**, 8017 (1996).
[17]J. E. Daniels, W. Jo, J. Rödel, D. Rytz, and W. Donner, Appl. Phys. Lett. **98**, 252904 (2011).
[18]C. Ma, X. Tan, E. Dul'kin, and M. Roth, J. Appl. Phys. **108**, 104105 (2010).
[19]J. Yao, L. Yan, W. Ge, L. Luo, J. Li, D. Viehland, Q. Zhang, and H. Luo, Phys. Rev. B **83**, 054107 (2011).
[20]Y. Hiruma, Y. Imai, Y. Watanabe, H. Nagata, and T. Takenaka, Appl. Phys. Lett. **92**, 262904 (2008).
[21]L. Pardo, E. Mercadelli, A. Garcia, K. Brebol, and C. Galassi, IEEE Trans. Ultrason. Ferroelectr. Freq. Control **58**, 1893 (2011).
[22]S. Teranishi, M. Suzuki, Y. Noguchi, M. Miyayama, C. Moriyoshi, Y. Kuroiwa, K. Tawa, and S. Mori, Appl. Phys. Lett. **92**, 182905 (2008).
[23]D. Viehland, S. J. Jang, L. E. Cross, and M. Wuttig, J. Appl. Phys. **68**, 2916 (1990).
[24]Z. Kutnjak, C. Filipic, R. Pirc, A. Levstik, R. Farhi, and M. El Marssi, Phys. Rev. B **59**, 294 (1999).
[25]W. Jo, S. Schaab, E. Sapper, L. A. Schmitt, H.-J. Kleebe, A. J. Bell, and J. Rödel, J. Appl. Phys. **110**, 074106 (2011).
[26]V. Bobnar, Z. Kutnjak, R. Pirc, and A. Levstik, Phys. Rev. B **60**, 6420 (1999).
[27]Z.-G. Ye and H. Schmid, Ferroelectrics **145**, 83 (1993).
[28]Y. Hiruma, H. Nagata, and T. Takenaka, J. Appl. Phys. **105**, 084112 (2009).
[29]T. Takenaka, H. Nagata, and Y. Hiruma, Jpn. J. Appl. Phys. **47**, 3787 (2008).
[30]K. Wojcik and A. Aleksandrowicz, Ferroelectrics **89**, 243 (1989).
[31]Y. Xi, C. Zhili, and L. E. Cross, Ferroelectrics **54**, 163 (1984).
[32]J. Jeong and Y. Han, J. Electroceram. **17**, 1051 (2006).
[33]E.-M. Anton, W. Jo, D. Damjanovic, and J. Rödel, J. Appl. Phys. **110**, 094108 (2011).

[34]W. Liu and C. A. Randall, J. Am. Ceram. Soc. **91**, 3245 (2008).
[35]W. Liu and C. A. Randall, J. Am. Ceram. Soc. **91**, 3251 (2008).
[36]H. Matsudo, K. Kakimoto, and I. Kagomiya, Jpn. J. Appl. Phys. **49**, 09MC07 (2010).
[37]S. T. Zhang, A. B. Kounga, E. Aulbach, and Y. Deng, J. Am. Ceram. Soc. **91**, 3950 (2008).
[38]E. Dul'kin, E. Mojaev, M. Roth, S. Greicius, and T. Granzow, Appl. Phys. Lett. **92**, 012904 (2008).
[39]E. V. Colla and M. B. Weissman, Phys. Rev. B **72**, 104106 (2005).
[40]P. M. Gehring, K. Ohwada, and G. Shirane, Phys. Rev. B **70**, 014110 (2004).
[41]E. V. Colla, D. Vigil, J. Timmerwilke, M. B. Weissman, D. D. Viehland, and B. Dkhil, Phys. Rev. B **75**, 214201 (2007).
[42]M. Foeth, P. Stadelmann, and M. Robert, Physica A **373**, 439 (2007).
[43]A. B. Kounga, T. Granzow, E. Aulbach, M. Hinterstein, and J. Rödel, J. Appl. Phys. **104**, 024116 (2008).